AIP | Applied Physics Letters

Modulation doping in ZnO nanorods for electrical nanodevice applications

Jinkyoung Yoo, Chul-Ho Lee, Yong-Joo Doh, Hye Seong Jung, and Gyu-Chul Yi

Citation: Applied Physics Letters **94**, 223117 (2009); doi: 10.1063/1.3148666
View online: http://dx.doi.org/10.1063/1.3148666
View Table of Contents: http://scitation.aip.org/content/aip/journal/apl/94/22?ver=pdfcov
Published by the AIP Publishing

Modulation doping in ZnO nanorods for electrical nanodevice applications

Jinkyoung Yoo,[1] Chul-Ho Lee,[1] Yong-Joo Doh,[1] Hye Seong Jung,[1] and Gyu-Chul Yi[2,a)]
[1]*Department of Materials Science and Engineering, POSTECH, San-31 Hyoja-dong, Pohang, Gyeongbuk 790-784, Republic of Korea*
[2]*National Creative Research Initiative Center for Semiconductor Nanorods, Department of Physics and Astronomy, Seoul National University, Seoul 151-747, Republic of Korea*

(Received 21 April 2009; accepted 13 May 2009; published online 4 June 2009)

We introduce a modulation-doping method to control electrical characteristics of ZnO nanorods. Compared with a conventional homogeneous doping method, the modulation-doping method generates localized doping layers along the circumference in ZnO nanorods, useful for many device applications. Here, we investigated electrical, structural, and optical characteristics of Ga-doped ZnO nanorods with the dopant modulation layers. Electrical conductivity of ZnO nanorods was controlled by changing either dopant mole fraction or the number of modulation-doped layers. Furthermore, the modulation-doped nanorod field effect transistors exhibited precisely controlled conductance in the order of magnitude without degradation of electron mobility. The effects of the doping on structural and optical characteristics of the nanorods are also discussed. © *2009 American Institute of Physics*. [DOI: 10.1063/1.3148666]

Recent progress in the growth of one-dimensional (1D) semiconductor nanostructures has provided significant opportunities for electronic and photonic nanodevice applications.[1,2] For the device fabrications, the electrical characteristics of semiconductor nanomaterials must be precisely controlled by impurity doping. Recent reports have shown that conductivity control by impurity doping in semiconductor nanomaterials is more problematic than in thin-film technology. Dopant incorporation during conventional homogeneous doping process causes a change in the nanowire growth direction, resulting in structural deformation.[3,4] In addition, unintentional defect formation during the process results in a significant decrease in the charge carrier mobility and can be the source of defect emission in the optical spectra.[5,6] Delta-doping process, which generate dopant atoms that are confined within a few atomic layers, have been widely used for fabricating modulation-doped thin-film heterostructures.[7] For 1D semiconductor nanostructures, the modulation-doping process forms dopant layers on the surfaces of the 1D nanostructures, which can show a more significantly enhanced modulation-doping effect due to their high surface to volume ratio.[8]

ZnO 1D nanostructures, including nanorods and nanowires, have been used in many electronic device applications. For example, transparent conducting ZnO thin films have been widely used as window electrodes for flat panel displays, touch panels, and solar cells, because of their excellent optical transparency and controllable electrical conductivity. Conventional ZnO thin films have been studied as semiconducting channels in thin-film transistors for electronic circuit applications. However, the transparent transistor applications are limited by poor device performance resulting from difficulty in preparing high-quality ZnO materials on glass substrates. An alternative approach is to use single crystal ZnO nanorods, which have a high charge carrier mobility and a low defect density, as building blocks for nanoscale electronics.[9–11] For the nanodevice applications, precise control of conductivity is required. Ga is well-known as an *n*-type dopant in ZnO and has been employed to increase the conductivity of ZnO nanorods and nanowires.[4,6,12] However, previous studies employing homogeneous doping of Ga in ZnO 1D nanostructures have reported unintentional effects, including an optical degradation[6,12] and structural deformation.[4,6] Here, we report on the modulation-doping technique to control electrical characteristics of ZnO nanorods for field effect transistor (FET) applications.

Ga-doped ZnO nanorods were grown on a Si (100) substrate using a low-pressure metal-organic chemical vapor deposition system without a metal catalysts. Except for gas interruption, the growth conditions and procedures of Ga-doped ZnO nanorods were practically identical to those used for growing the nominally undoped ZnO nanorods, as described elsewhere in the literature.[13] As shown in Fig. 1(a), the modulation-doping process introduces gas flow interruption during the growth. After growth of undoped ZnO nanorods, diethyl-Zn (DEZn) and oxygen gas flows were then halted and trimethyl-Ga (TMGa) was introduced into the reactor for a typical duration of 5 s. After this, DEZn was introduced into the reactor for 2 s, then oxygen was supplied together with the DEZn for a further 5 s in order to deposit a ZnO capping layer without forming a gallium oxide.

Optical and structural characterization of the nanorods was carried out by using photoluminescence (PL) spectroscopy, scanning electron microscopy (SEM), and transmission electron microscopy (TEM) as details in the measurements are reported elsewhere.[14,15]

FETs fabricated from individual ZnO nanorods were studied in order to investigate the electrical characteristics of Ga-modulation-doped ZnO nanorods. The device fabrication method was quite similar to that in our previous report except we did not use the post thermal annealing process here,[10] as it may induce interdiffusion of the dopants. Although thermal annealing was not employed, good Ohmic contacts on the doped nanorods were formed using the Ti/Au layer. All electrical measurements were performed in a vacuum chamber at 10^{-6} Torr and at room temperature in order to minimize the effect of environmental gases on the

a)Electronic mail: gcyi@snu.ac.kr.

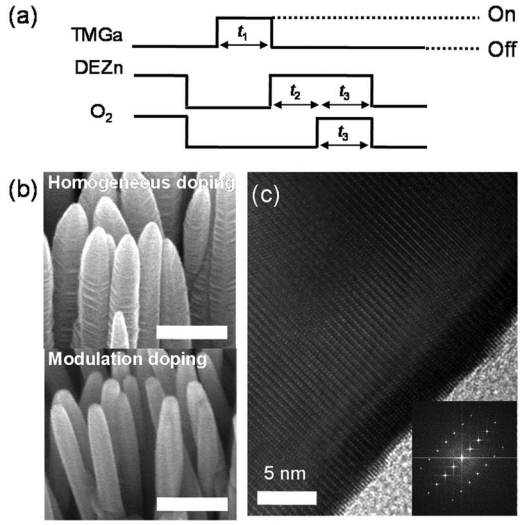

FIG. 1. (a) Schematic of the modulation-doping process for growth of Ga-modulation-doped ZnO nanorods. Temporal operation of the metal-organic vapor and gas flow is depicted in sequence, from top to bottom. (b) Typical field emission (FE)-SEM images of homogeneously Ga-doped ZnO nanorods (top) and Ga-modulation-doped ZnO nanorods (bottom). The scale bar indicates 200 nm. (c) Typical HR-TEM image of modulation-doped ZnO nanorods. The inset shows the selective area electron diffraction pattern of a Ga-modulation-doped nanorod stem.

electrical characteristics of the nanorods, as previously reported.[16]

The surface morphology of the ZnO nanorods was investigated using SEM and TEM. As shown in Fig. 1(b), smooth surfaces were observed for Ga-modulation-doped ZnO nanorods, in contrast to roughened sidewalls for the homogeneously doped nanorods. The morphological change in the 1D semiconductor nanostructures during the homogeneous doping was consistent with previous work.[3,4,17] In addition to the morphological change, previous studies reported a change in the nanorod growth direction from [0001] to $[10\bar{1}2]$ during continuous Ga incorporation, and concurrent structural deformation.[4] In contrast, for modulation-doped ZnO nanorods, a clear single crystalline lattice without any structural defects was observed from the high-resolution (HR)-TEM image, as shown in Fig. 1(c). Selective area electron diffraction patterns also confirmed the single crystalline nature of the modulation-doped ZnO nanorods.

The electrical characteristics of the doped ZnO nanorods were investigated by measuring the current-voltage (I_{ds}-V_{ds}) characteristics of nanorod FETs. Figure 2 shows the typical

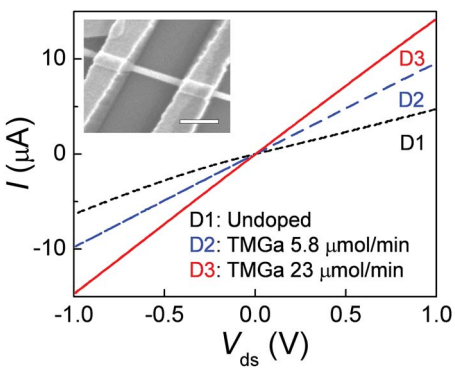

FIG. 2. (Color online) I_{ds}-V_{ds} characteristic curves of individual ZnO nanorod devices with TMGa flow rates of 0, 5.8, and 23 μmol/min. The inset is the typical FE-SEM image of the nanorod device where scale bar is 500 nm.

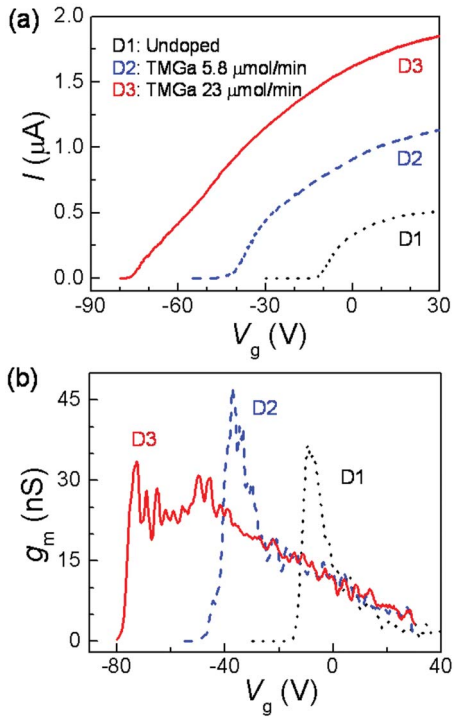

FIG. 3. (Color online) (a) I_{ds}-V_g transfer characteristic curves of individual ZnO nanorod devices with TMGa flow rates of 0, 5.8, and 23 μmol/min. V_{ds} was fixed at 0.1 V. (b) Corresponding transconductance curve at V_{ds}=0.1 V.

I_{ds}-V_{ds} characteristics for a series of doped ZnO nanorod FETs with different TMGa mole fractions. The most significant change due to the Ga-modulation-doping was the increased overall conductance with increasing TMGa mole fraction. Neglecting contact resistances, the conductivity (σ) of the nominally undoped nanorods increased from 6.3 ± 2.1 to 14.5 ± 2.8 and 13.6 ± 3.1 S/cm for the doped nanorods with TMGa flow rate of 5.8 and 23 μmol/min, respectively. In addition, the conductance of the doped ZnO nanorods could be controlled by the number of modulation-doping cycles. For the doped ZnO nanorods with a TMGa flow rate of 5.8 μmol/min, the conductance was 6.67 μS for one cycle of modulation-doped layer deposition, and 15.1 μS for four cycles of deposition. The systematic increase in the overall conductance shows that the carrier concentration in the doped nanorods can be controlled by changing either the TMGa mole fraction or the number of cycles of the modulation-doping process.

Further electrical characteristics of the doped ZnO nanorods were investigated by measuring the gate bias (V_g) dependent current (I_{ds}) characteristics (transfer characteristics) of the nanorod FETs. Figure 3(a) shows I_{ds}-V_g curves of undoped and doped ZnO nanorod FETs. For the doped ZnO nanorod FETs, the saturation current increased, and the threshold voltage (V_{th}) shifted to the negative direction of the V_g-axis. The observation that V_{th} shift to a lower voltage for the doped nanorod FETs indicates that a larger V_g must be applied to deplete the carriers completely in the doped devices (D2 and D3) than that in the undoped ZnO nanorod (D1) devices. The saturation current level also increased with the dopant concentration since σ is proportional to the carrier concentration (n). Accordingly, a significant change in the I_{ds}-V_g characteristics was mainly attributed to the increased carrier concentration in the doped ZnO nanorods.

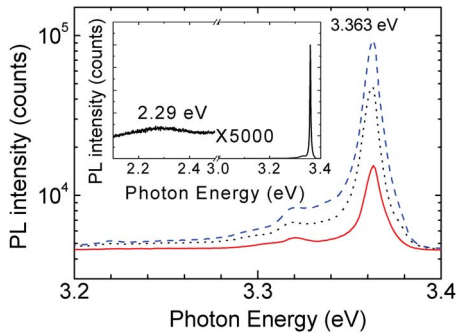

FIG. 4. (Color online) 10 K PL spectra of nominally undoped (black, dotted) and Ga-modulation-doped ZnO nanorods with TMGa flow rates of 5.8 (blue, dashed) and 23 μmol/min (red, solid). The inset shows very weak visible emission from Ga-modulation-doped nanorods with TMGa flow rate of 23 μmol/min.

Quantitative information on the carrier concentration of the doped nanorods was obtained using the expression of $n=C_gV_{th}/U$,[18] where C_g is the gate capacitance and $U=\pi\phi^2L/4$ is a total volume of the nanorod segment between two electrodes. The capacitive coupling between the back-gate electrode and the ZnO nanorods was not significantly changed by the geometrical parameters of L and ϕ. After analyzing the I_{ds}-V_g characteristics of a total of 16 devices, we estimated $n=1.8(\pm0.4)\times10^{18}$ cm^{-3} for the nominally undoped ZnO nanorods and $3.9(\pm1.0)\times10^{18}$ cm^{-3} and $4.7(\pm0.5)\times10^{18}$ cm^{-3} for doped ones with TMGa flow rates of 5.8 and 23 μmol/min, respectively.

In addition to the carrier concentration, the carrier mobility is another key parameter that is affected by the doping concentration. This was estimated by analyzing the transconductance ($g_m=dI_{ds}/dV_g$), resulting in the peaks near the subthreshold region shown in Fig. 3(b). From the peak in g_m, the corresponding carrier mobility determined from the $\mu=L^2g_m/C_gV_{ds}$ was 31.1 ± 8.0 for the undoped ZnO nanorods, and 41.7 ± 8.6 and 35.5 ± 3.4 cm^2/V s for the doped ones with TMGa flow rates of 5.8 and 23 μmol/min, respectively, indicating that the formation of the Ga-modulation-doping layer did not reduce the charge carrier mobility.

The effect of Ga-modulation-doping on the optical characteristics of the doped ZnO nanorods was investigated by performing the low temperature PL spectroscopy. Figure 4 shows the PL spectra of the nominally undoped and doped ZnO nanorods grown at the two different TMGa flow rates of 5.8 and 23 μmol/min measured at 10 K. All the PL spectra were dominated by near-band-edge emission, while visible emission from deep levels was negligible (see the inset). The dominant emission peak at 3.363 eV was attributed to neutral donor bound exciton emission (I_4),[19] and the small peak at 3.320 eV was attributed to the two-electron satellite of the donor bound exciton emission.[20] Although there was no significant change in the spectral shape even for the heavily doped nanorods, the lightly doped ZnO nanorods exhibited much higher PL intensity than either the undoped or the heavily doped ZnO nanorods. The increase in the PL intensity observed in the lightly doped nanorods compared to the undoped ones was due to an increase in the donor concentration. However, when the dopant concentration was too high, as in the heavily doped nanorods, the PL intensity fell because of the compensation effect, which induced defect complexes or formed nonradiative defects due to the excess Ga atoms.[21] The compensation effect could be avoided by increasing the number of modulation-doping layers rather than increasing the TMGa mole fraction.

In summary, a Ga modulation-doping technique was employed to control the conductivity of ZnO nanorods and the electrical characteristics of nanorod FETs. The overall conductance of ZnO nanorods was controlled precisely by changing the dopant concentration and the number of cycles in the modulation-doping process. The modulation-doped ZnO nanorod FETs exhibited systematic changes in conductance and threshold voltage with the TMGa mole fraction used in the growth of the nanorods. Furthermore, high performance operation was achieved without any significant degradation of the charge carrier mobility or the transconductance. We believe that this modulation-doping technique offers a reliable route for controlling the conductivity of semiconductor nanorods with high precision, and without negatively affecting other electrical and optical characteristics.

This study was financially supported by the National Creative Research Initiative Project (Grant No. R16-2004-004-01001-0) of the Korea Science and Engineering Foundations (KOSEF).

[1] C. M. Lieber and Z. L. Wang, MRS Bull. **32**, 99 (2007).
[2] C. Thelander, P. Agarwal, S. Brongersma, J. Eymery, L. F. Feiner, A. Forchel, M. Scheffler, W. Riess, B. J. Ohlsson, U. Gösele, and L. Samuelson, Mater. Today **9**, 28 (2006).
[3] H. J. Fan, B. Fuhrmann, R. Scholz, C. Himcinschi, A. Berger, H. Leipner, A. Dadgar, A. Krost, S. Christiansen, U. Gösele, and M. Zacharias, Nanotechnology **17**, S231 (2006).
[4] G.-D. Yuan, W.-J. Zhang, J.-S. Jie, X. Fan, J.-X. Tang, I. Shafig, Z.-Z. Ye, C.-S. Lee, and S.-T. Lee, Adv. Mater. (Weinheim, Ger.) **20**, 168 (2008).
[5] J. Zhong and G. M. Stocks, Nano Lett. **6**, 128 (2006).
[6] C.-L. Hsu, Y.-R. Lin, S.-J. Chang, T.-H. Lu, T.-S. Lin, S.-Y. Tsai, and I.-C. Chen, J. Electrochem. Soc. **153**, G333 (2006).
[7] E. F. Schubert, *Delta Dopings in Semiconductors* (Oxford University Press, New York, 1996).
[8] W. I. Park, J. Korean Phys. Soc. **53**, L1759 (2008).
[9] W. I. Park, J. S. Kim, G.-C. Yi, and H.-J. Lee, Adv. Mater. (Weinheim, Ger.) **17**, 1393 (2005).
[10] W. I. Park, J. S. Kim, G.-C. Yi, M. H. Bae, and H.-J. Lee, Appl. Phys. Lett. **85**, 5052 (2004).
[11] M. S. Arnold, P. Avouris, Z. W. Pan, and Z. L. Wang, J. Phys. Chem. B **107**, 659 (2003).
[12] J. Zhong, S. Muthukumar, Y. Chen, Y. Lu, H. M. Ng, W. Jiang, and E. L. Garfunkel, Appl. Phys. Lett. **83**, 3401 (2003).
[13] W. I. Park, D. H. Kim, S. W. Jung, and G.-C. Yi, Appl. Phys. Lett. **80**, 4232 (2002).
[14] Y. J. Hong, H. S. Jung, J. Yoo, Y.-J. Kim, C.-H. Lee, M. Kim, and G.-C. Yi, Adv. Mater. (Weinheim, Ger.) **21**, 222 (2009).
[15] W. I. Park, Y. H. Jun, S. W. Jung, and G.-C. Yi, Appl. Phys. Lett. **82**, 964 (2003).
[16] C.-H. Lee, J. Yoo, Y.-J. Doh, and G.-C. Yi, Appl. Phys. Lett. **94**, 043504 (2009).
[17] M. Kim, Y. J. Hong, J. Yoo, G.-C. Yi, G.-S. Park, K. Ki-jeong, and H. Chang, Phys. Status Solidi RRL **2**, 197 (2008).
[18] R. Martel, T. Schmidt, H. R. Shea, T. Hertel, and Ph. Avouris, Appl. Phys. Lett. **73**, 2447 (1998).
[19] B. K. Meyer, H. Alves, D. M. Hofmann, W. Kriegseis, D. Forster, F. Bertram, J. Christen, A. Hoffmann, M. Straßburg, M. Dworzak, U. Haboeck, and A. V. Rodina, Phys. Status Solidi B **241**, 231 (2004).
[20] A. Teke, Ü. Özgür, S. Doğan, X. Gu, H. Morkoç, B. Nemeth, and J. Nause, Phys. Rev. B **70**, 195207 (2004).
[21] H. J. Ko, Y. F. Chen, S. K. Hong, H. Weinsch, T. Yao, and D. C. Look, Appl. Phys. Lett. **77**, 3761 (2000).